AD-750 611

OPTOELECTRONIC ELECTRON EMITTER

Horst E. Schade, et al

RCA Laboratories

Prepared for:

Army Electronics Command

October 1972

AD

RESEARCH AND DEVELOPMENT TECHNICAL REPORT
ECOM-0059-3

OPTOELECTRONIC ELECTRON EMITTER

SEMIANNUAL REPORT

BY

H. SCHADE, H. F. LOCKWOOD, AND H. KRESSEL

OCTOBER 1972

SPONSORED BY: ADVANCED RESEARCH PROJECTS AGENCY
ARPA ORDER NO. 1686

DISTRIBUTION STATEMENT
Approved for public release; distribution unlimited.

ECOM

UNITED STATES ARMY ELECTRONICS COMMAND · FORT MONMOUTH, N.J.

CONTRACT DAAB07-71-C-0059
RCA LABORATORIES
PRINCETON, N. J. 08540

28

NOTICES

Disclaimers

The findings in this report are not to be construed as an official Department of the Army position, unless so designated by other authorized documents.

The citation of trade names and names of manufacturers in this report is not to be construed as official Government indorsement or approval of commercial products or services referenced herein.

Disposition

Destroy this report when it is no longer needed. Do not return it to the originator.

UNCLASSIFIED

Security Classification

DOCUMENT CONTROL DATA - R & D

(Security classification of title, body of abstract and indexing annotation must be entered when the overall report is classified)

1. ORIGINATING ACTIVITY (Corporate author) RCA Laboratories Princeton, New Jersey 08540	2a. REPORT SECURITY CLASSIFICATION Unclassified 2b. GROUP N/A

3. REPORT TITLE

OPTOELECTRONIC ELECTRON EMITTER

4. DESCRIPTIVE NOTES (Type of report and inclusive dates)

Semiannual Report 1 January 1972 to 30 June 1972

5. AUTHOR(S) (First name, middle initial, last name)

Horst E. Schade, Henry Kressel, Harry F. Lockwood

6. REPORT DATE October 1972	7a. TOTAL NO. OF PAGES ~~29~~ 28	7b. NO. OF REFS 10
8a. CONTRACT OR GRANT NO. DAAB07-71-C-0059 b. PROJECT NO. 79 1021 7034401 c. d.	9a. ORIGINATOR'S REPORT NUMBER(S) PRRL-72-CR-40 9b. OTHER REPORT NO(S) (Any other numbers that may be assigned this report) ECOM-0059-3	

10. DISTRIBUTION STATEMENT

Approved for public release; distribution unlimited.

11. SUPPLEMENTARY NOTES ARPA Order No. 1686	12. SPONSORING MILITARY ACTIVITY United States Army Electronics Command. Fort Monmouth, N.J. 07703 AMSEL-TL-BA

13. ABSTRACT

The electron energy distribution of a semiconductor cold-cathode based on negative electron affinity has been measured for the first time. The half-width of the energy distribution of electrons, emitted from a GaAs-(AlGa)As structure, has been found to be 160 meV which is distinctly narrower than that for a conventional thermionic cathode. The measured half-width is in fair agreement with calculations that take into account energy losses suffered by the electrons in the space-charge region below the surface. In order to improve surface escape probabilities, various surface preparations have been investigated by a series of photoemission experiments. In addition to ⟨100⟩ GaAs surfaces studied thus far, ⟨111B⟩ surfaces were also activated. However, our previous values on surface escape probabilities could not be exceeded. Since emission efficiencies of negative electron affinity emitters depend strongly on the electron diffusion length in the emitting material, independent measurements of the diffusion length have been made by using a laser beam and an α-particle beam technique. Our earlier results on GaAs:Ge derived from photoemission measurements were corroborated. Furthermore, the diffusion length in higher doped material ($\sim 10^{19} cm^{-3}$) has been found to be still rather long (~5 μm). The use of this highly doped material in cold-cathodes thus may reduce the series resistance of the diodes as well as the energy spread of the emitted electrons, without a loss in emission efficiency due to reduced diffusion lengths. After having obtained excellent shelf life of cold-cathode efficiency in a sealed tube (~2% for 2 months), preliminary results on long-term operation in a sealed tube indicate that the cathode degradation rate compares favorably with previous results found in continuously pumped tubes. The transition to sealed tubes, therefore, does not seem to adversely affect cold-cathode operation.

DD FORM 1 NOV 65 1473

UNCLASSIFIED

Security Classification

14 KEY WORDS	LINK A		LINK B		LINK C	
	ROLE	WT	ROLE	WT	ROLE	WT
Electron Emission						
Electron Emitters						
Semiconductor Cold-Cathodes						
Semiconductor Cold-Cathode Structures						
Negative Electron Affinity						
Low Work Function						
GaAs						
(AlGa)As						

TECHNICAL REPORT ECOM-0059-3
OCTOBER 1972

REPORTS CONTROL SYMBOL
OSD-1366

OPTOELECTRONIC ELECTRON EMITTER

SEMIANNUAL REPORT

1 JANUARY 1972 TO 30 JUNE 1972

CONTRACT NO. DAAB07-71-C-0059 DA PROJECT NO. 7910217034401

ARPA ORDER NO. 1686 DATE OF CONTRACT: 10/21/70
PROGRAM CODE NO. OD10 AMOUNT OF CONTRACT: $61,500
CONTRACT EXPIRATION DATE: 31 DECEMBER 1972

DISTRIBUTION STATEMENT

Approved for public release; distribution unlimited.

PREPARED BY
H. SCHADE, PRINCIPAL INVESTIGATOR (TEL. EXT.: 2910)
H. F. LOCKWOOD
H. KRESSEL, PROJECT SCIENTIST AND SUPERVISOR (TEL. EXT.: 2427)

RCA LABORATORIES
TEL.: (609) 452-2700
PRINCETON, NEW JERSEY 08540

FOR

U. S. ARMY ELECTRONICS COMMAND, FORT MONMOUTH, NEW JERSEY 07703

FOREWORD

This Semiannual Report describes research performed at RCA Laboratories in the Materials Research Laboratory, J. J. Tietjen, Director. The Project Supervisor is H. Kressel. The Technical Staff consisted of Dr. H. Schade (Principal Investigator), Dr. H. F. Lockwood, and H. Nelson (Consultant). B. Smith is the Army COTR. This research was supported by the Advanced Research Projects Agency of the Department of Defense and was monitored by the U. S. Army Electronics Command (ECOM) under Contract No. DAAB07-71-C-0059. The authors wish to thank V. M. Cannuli, D. B. Gilbert, and A. E. White for skillful technical assistance. Dr. M. Ettenberg contributed to this work under RCA funding.

ABSTRACT

The electron energy distribution of a semiconductor cold-cathode based on negative electron affinity has been measured for the first time. The half-width of the energy distribution of electrons, emitted from a GaAs-(AlGa)As structure, has been found to be 160 meV which is distinctly narrower than that for a conventional thermionic cathode. The measured half-width is in fair agreement with calculations that take into account energy losses suffered by the electrons in the space-charge region below the surface.

In order to improve surface escape probabilities, various surface preparations have been investigated by a series of photoemission experiments. In addition to ⟨100⟩ GaAs surfaces studied thus far, ⟨111B⟩ surfaces were also activated. However, our previous values on surface escape probabilities could not be exceeded.

Since emission efficiencies of negative electron affinity emitters depend strongly on the electron diffusion length in the emitting material, independent measurements of the diffusion length have been made by using a laser beam and an α-particle beam technique. Our earlier results on GaAs:Ge derived from photoemission measurements could be corroborated. Furthermore, the diffusion length in higher doped material ($\sim 10^{19} cm^{-3}$) has been found to be still rather long ($\sim 5\ \mu m$). The use of this highly doped material in cold-cathodes thus may reduce the series resistance of the diodes as well as the energy spread of the emitted electrons, without a loss in emission efficiency due to reduced diffusion lengths.

After having obtained excellent shelf life of cold-cathode efficiency in a sealed tube (~2% for 2 months), preliminary results on long-term operation in a sealed tube indicate that the cathode degradation rate compares favorably with previous results found in continuously pumped tubes. The transition to sealed tubes, therefore, does not seem to adversely affect cold-cathode operation.

TABLE OF CONTENTS

Section		Page
I.	INTRODUCTION	1
II.	ENERGY DISTRIBUTION OF ELECTRONS EMITTED FROM A NEGATIVE ELECTRON AFFINITY GaAs-(AlGa)As COLD-CATHODE	2
III.	SURFACE ESCAPE STUDIES	8
IV.	DIFFUSION LENGTH MEASUREMENTS	10
	A. Diffusion Length Measurement Using Laser Scan	10
	B. Diffusion Length Measurement Using α-Particles	12
V.	OPERATION IN SEALED TUBES	16
VI.	CONCLUSIONS	17
VII.	FUTURE PLANS	18
REFERENCES		19

Preceding page blank

LIST OF ILLUSTRATIONS

Figure		Page
1.	Energy band diagram of an optoelectronic semiconductor cold-cathode	2
2.	Retarding field technique for electron energy distribution measurement	4
3.	Energy distribution of electrons emitted from a GaAs cold-cathode; also shown in the same energy scale is the spatial dependence of the conduction band edge adjacent to the emitting surface	5
4.	Energy distribution of electrons reaching the surface, but prior to being emitted	6
5.	Energy distribution of electrons emitted from a GaAs cold-cathode and from a conventional thermionic cathode (Maxwell-Boltzmann distribution). The curves have been matched at their maxima and have been normalized to equal total emission	7
6.	Scanning electron micrographs of a $\langle 100 \rangle$ GaAs surface (a) before and (b) after heating in vacuum to about 600°C	9
7.	Scanning laser beam method for electron diffusion length measurement	11
8.	Short-circuit current as a function of the thickness of the p-layer which is illuminated by the laser beam	13

I. INTRODUCTION

This research study is a continuation of an effort to develop a solid-state electron emitter which has been started under a previous one-year contract entitled "Optoelectronic Electron Emitter." This study was motivated by the need for electron emitters that have a narrower electron velocity distribution than present hot cathodes, can be readily modulated, are capable of being fabricated in array form, have long life, and do not require heat shielding which complicates tube construction.

During the first year of the contract period, we developed a greatly improved cold-cathode emitter based on the use of liquid-phase epitaxy, (AlGa)As-GaAs heterojunctions, and negative electron affinity GaAs surfaces (1). An important part of the device is the lateral confinement of the current flow to the desired emitting surface by a novel fabrication technique involving the selective diffusion of Zn. It was shown for the first time that III-V semiconductor cold-cathodes are capable of dc operation at efficiencies and emission-current densities of practical interest; record values were obtained which exceeded the objectives of this program. Sustained efficiency values of 1.9% were obtained with emission currents of 190 μA. The dc emission-current densities ranged from 0.1 to 0.4 A/cm^2. Pulsed operation with efficiencies of 4% was obtained, and emission-current densities as high as 7 A/cm^2 were measured.

Some of the major factors affecting cathode life were studied. The release of impurity atoms from the anode as a result of electron-stimulated desorption was a major problem, since these impurities are physically absorbed on the cathode surface, thus reducing the negative electron affinity. This effect can be minimized by a number of techniques, including low voltages, magnetic-field deflection, and "clean" semiconductor anodes.

A key property of the semiconductor cold-cathode, namely the energy distribution of the emitted electrons, must still be measured. Therefore, before any further optimizing of cold-cathode performance in regard to efficiency and life, the first goal of the second contract period was to verify that the electron energy distribution of a semiconductor cold-cathode is, in fact, narrower than that of a conventional thermionic cathode. In addition, we will describe further efforts to increase the cathode emission efficiencies by improving the surface escape probability and controlling the electron diffusion lengths. Finally, we will report on cold-cathode operation in sealed tubes, which ultimately determines feasibility of these cold-cathodes in practical devices.

II. ENERGY DISTRIBUTION OF ELECTRONS EMITTED FROM A NEGATIVE ELECTRON AFFINITY GaAs-(AlGa)As COLD-CATHODE

The optoelectronic cold-cathode structure consists of an electroluminescent diode of higher bandgap material, (AlGa)As:Si, covered with a thin top layer of lower bandgap material, GaAs:Ge, whose surface is activated to a condition of negative electron affinity (see Figure 1). Under such a condition, the work function has been lowered to a value smaller than the bandgap of the top GaAs layer, and electrons generated in this layer need no additional kinetic energy in order to be emitted into vacuum. Electron emission from the structure shown in Figure 1 is obtained as follows.

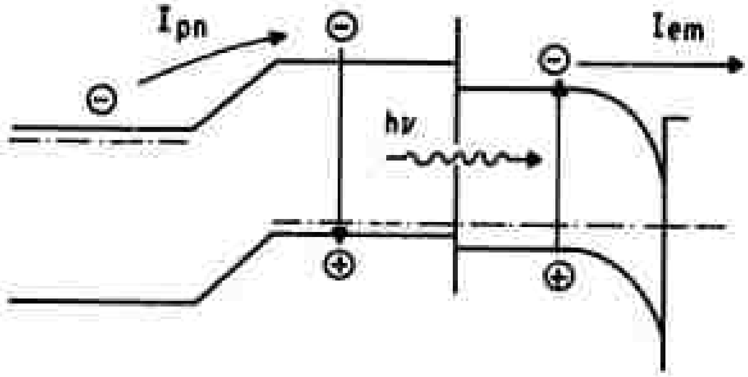

Figure 1. Energy band diagram of an optoelectronic semiconductor cold-cathode.

Under forward bias, electrons are injected into the p-type (AlGa)As region where they recombine radiatively. The emitted photons ($h\nu$ = 1.41 to 1.6 eV) are strongly absorbed in the highly p-type GaAs surface layer (E_g = 1 42 eV), thus creating electron-hole pairs. A substantial number of the electrons that diffuse to the surface are then emitted into vacuum from the negative electron affinity surface.

Since such semiconductor cold-cathodes operate at room temperature, they are expected to have a narrower energy distribution of the emitted electrons than conventional thermionic cathodes operating at about 1000 K. This would represent a major advantage in all beam focussing and imaging applications and would result also in reduced beam-discharge lag in camera tubes, for instance. A second advantage implied by cold-cathode emission is lower noise which may lead to higher signal sensitivity of devices incorporating cold-cathodes rather than thermionic cathodes. Finally, devices incorporating cold-cathodes require no heat shielding, which greatly simplifies the construction of infrared-sensing devices.

We have concentrated our efforts on experimentally verifying the narrow energy distribution of a negative electron affinity cold-cathode which -- to our knowledge -- has not been measured before. In order to do this measurement, we have designed and constructed a tube to apply a retarding field technique. The principle of this technique is shown in Figure 2, in the upper portion in terms of the energy band diagram of the electrodes involved, and in the lower portion schematically in terms of the actual electrodes in the tube. The cathode is surrounded by a hemispherically shaped grid electrode, beyond which a collector electrode is located. The retarding voltage on the grid is varied in such a way that only electrons above a certain kinetic energy can reach the grid and subsequently be collected by the collector. The collected current as a function of the retarding voltage contains the information on the energy distribution of the emitted electrons. By using lock-in techniques and thus differentiating the collected current with respect to the retarding voltage, the energy distribution can be readily displayed.

The construction of the retarding field electrode was led by two considerations: (1) The electrode was shaped into a hemispherical shell in order to preserve the angular distribution of the electrons as they are emitted. (2) The electrode transmits electrons only through a small hole directly opposite to the emitting surface. Thus, the electrons are selected only from a small solid angle in which field distortions can be neglected.

In our experiments, we used a GaAs-(AlGa)As heterojunction structure operating with direct electron injection (1). We used this structure because it allowed us to obtain a smaller emitting area than with the optoelectronic structure. A small emitting area, approaching as closely as possible a true point source, is essential to obtain reliable energy distribution data. The experimental results equally should hold for an optoelectronic emitter, since the supply of electrons to be emitted consists, in both cases, of thermalized electrons in the Ge-doped p-type GaAs top layer of the structure. This will be experimentally determined at a later date.

The energy distribution of a sample exhibiting a total emission efficiency of 2% is shown in Figure 3. Also shown in the same energy scale is the spatial dependence of the lower conduction band edge in the surface region. The conclusion to be drawn from this figure is that essentially monoenergetic electrons reaching the bent band region become subject to a spread in their energy upon emission from the surface. The half-width of the measured energy distribution (solid line) was found to be 160 meV, which equals about 6 kT at room temperature. This half-width is distinctly smaller than that of a conventional thermionic cathode, which at 1000 K would give rise to a half-width 220 meV (see Figure 5).

Thus, we have obtained the first experimental proof that the energy distribution of a GaAs cold-cathode based on negative electron affinity is, indeed, narrower than in the case of conventional hot cathodes.

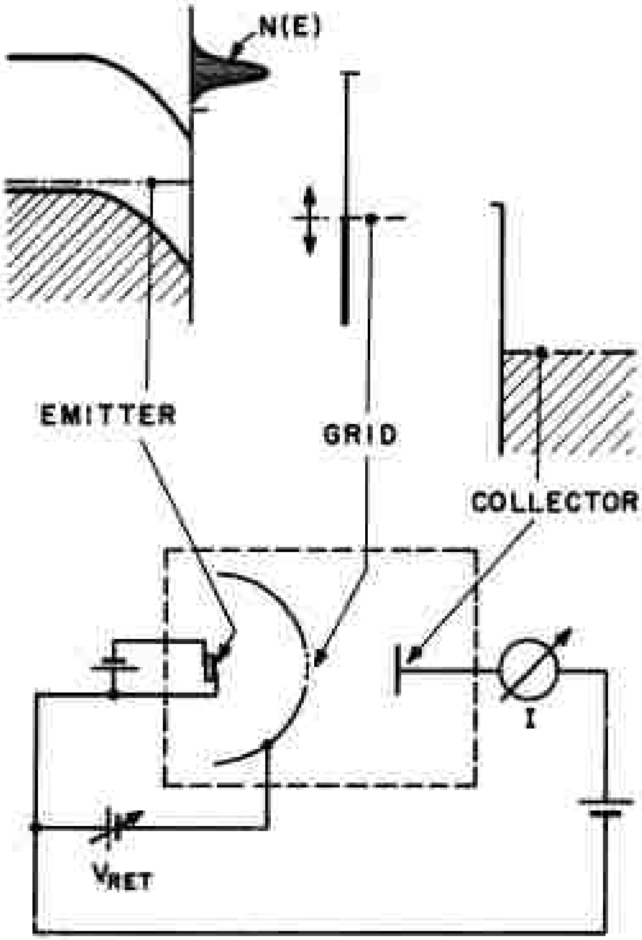

Figure 2. Retarding field technique for electron energy distribution measurement.

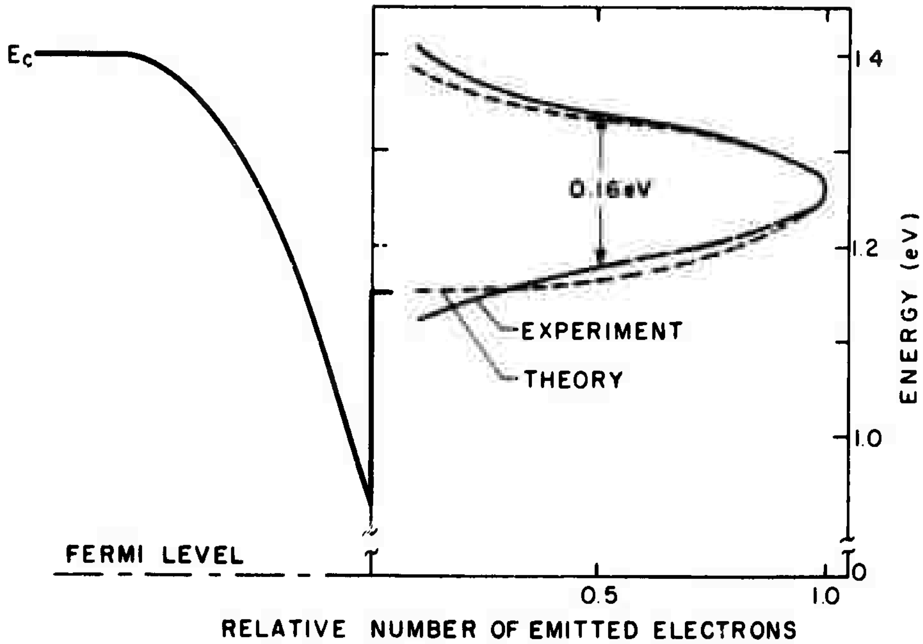

Figure 3. Energy distribution of electrons emitted from a GaAs cold-cathode; also shown in the same energy scale is the spatial dependence of the conduction band edge adjacent to the emitting surface.

However, the measured width of 6 kT requires some explanation, since it might seem larger than to be expected. Based on a model by Bartelink et al.(2), we have, therefore, calculated the energy distribution of the electrons being emitted from the semiconductor. Here one must consider that the electrons reaching the surface space charge region are accelerated by the internal electric field in this region, but at the same time become subject to energy losses to optical phonons. These interactions are characterized by a mean free electron path ℓ_p between two collisions with optical phonons and by an energy loss ΔE_p per collision. Besides these collision parameters, the total energy loss E_p of each electron depends on the number of collisions the electron suffers on its way to the surface. This number, in turn, is a function of the thickness d of the space charge region which is given by the doping concentration of the semiconductor material. The effect of doping on the energy distribution of electrons reaching the surface is illustrated in Figure 4. The curves shown here are calculated from a solution of the Boltzmann transport equation which has been given by Bartelink et al. (2) in general form and has been modified by us to the conditions of our present problem. Neglecting ionization losses of the electrons, this modified solution takes the form:

$$N(E_p) = \text{const.} \left[\left(\frac{V}{E_p}\right)^2 - \left(\frac{V}{E_p}\right)\right] \exp\left[\frac{3}{4}\left(\frac{d}{\ell_p}\right)^2 \frac{\Delta E_p}{E_p}\right] \qquad (1)$$

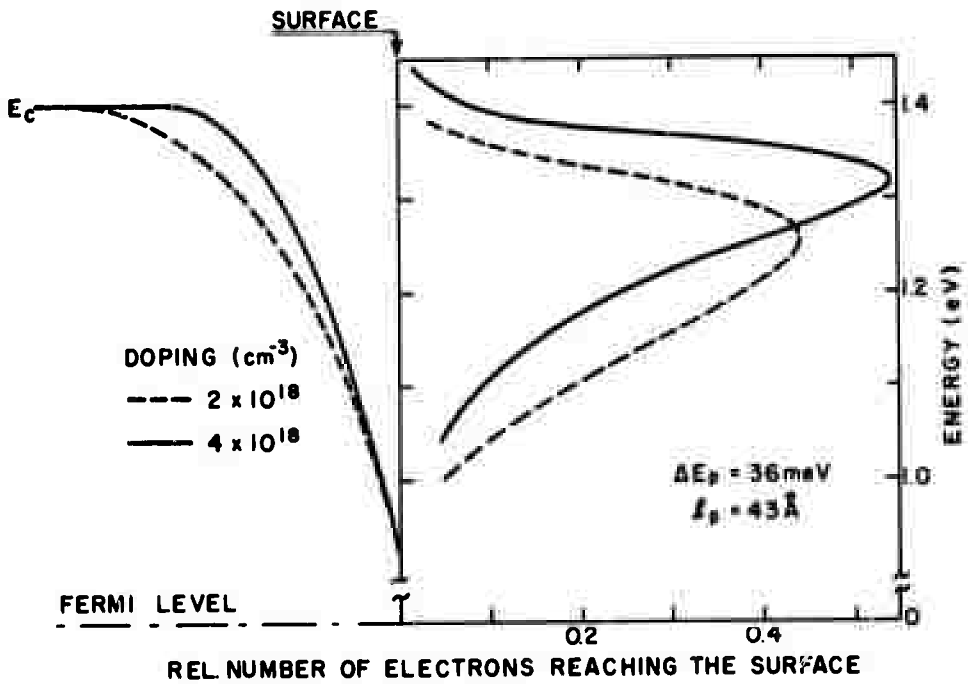

Figure 4. Energy distribution of electrons reaching the surface, but prior to being emitted.

assuming

$$V - E_p >> \frac{(F\ell_p)^2}{6\Delta E_p} \quad \text{and } F = \frac{V}{d} ,$$

where, in addition to the quantities mentioned above, V is the amount of band-bending and F is the electric field in the bent-band region.

By multiplying Eq.(1) with an energy-dependent surface escape probability P_W, one obtains the energy distribution of electrons being <u>emitted</u> from the surface, as shown by the dashed curve in Figure 3. This curve was obtained by assuming a work function of W = 1.15 eV for the cesiated GaAs surface and a simple step function potential barrier at the surface. For this barrier, P_W is given by

$$P_W = \frac{4\sqrt{V-E_p}\,\sqrt{E_g-W-E_p}}{(\sqrt{V-E_p} + \sqrt{E_g-W-E_p})^2} \qquad (2)$$

where E_g is the bandgap of the semiconductor material and W the work function of the cesiated surface (note that E_g > W for negative electron affinity).

The comparison between the experimental and theoretical energy distribution indicates that the measured half-width of about 6 kT is consistent with theoretical expectations. The remaining discrepancies between the two curves lie well within the limits of the experimental energy resolution.

Finally, in comparing the energy distributions emitted from a cold-cathode and a thermionic cathode we note, in addition to different half-widths, a significant difference in the shape of the distribution. This difference is illustrated in Figure 5 by showing our measured distribution and a Maxwell-Boltzmann distribution emitted from a thermionic cathode at 1000 K (3). While for thermionic cathodes there is a distinct exponential high energy tail, the cold-cathode distribution falls off rather sharply toward high electron energies, which is a considerable advantage in all beam-focussing and beam-landing considerations.

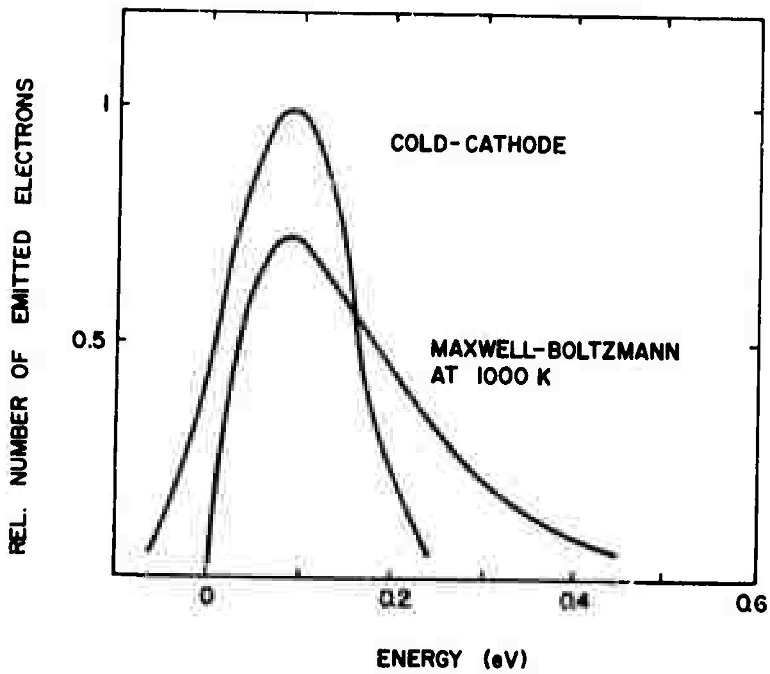

Figure 5. Energy distribution of electrons emitted from a GaAs cold-cathode and from a conventional thermionic cathode (Maxwell-Boltzmann distribution). The curves have been matched at their maxima and have been normalized to equal total emission.

III. SURFACE ESCAPE STUDIES

Our previous photoemission studies on liquid phase grown (4) GaAs:Ge indicated that the electron escape probabilities for our emitting surfaces are about a factor of 2 lower than the highest values reported for GaAs also grown by liquid phase epitaxy (5). Since the cold-cathode emission efficiency is directly proportional to the surface escape probability, and since we found the process of surface activation to depend on the surface treatment prior to mounting the sample into the vacuum chamber, we have started a series of photoemission experiments to investigate various surface preparations which might lead to an improved surface escape probability. Besides the usual etching in a mixture of H_2SO_4, H_2O_2, and H_2O, we tried a subsequent etch in H_2O_2, and also a heating in hydrogen prior to mounting the sample into the vacuum system. All these treatments led to about the same photosensitivities. We also tried *in situ* heating of the sample in hydrogen just prior to the activation process. But thereafter the photosensitivity was lower by a factor of two. We did find, however, that the original photosensitivity, 800 μA/lm in this case, could be restored after ion bombardment with cesium or oxygen, followed by a 15-minute annealing step. At the same time, the photosensitivity after this procedure was considerably more stable than before.

Furthermore, we studied ⟨111B⟩ GaAs surfaces which reportedly (5) exhibit higher escape probabilities than the ⟨100⟩ surfaces used thus far. While our previous results on ⟨100⟩ surfaces could be reproduced with ⟨111B⟩ surfaces, an improvement with these surfaces has not yet been found.

In connection with these surface studies, we also checked whether the usual heat cleaning of the surface in vacuum might produce any facetting. Heated and unheated ⟨100⟩ surfaces were tested by scanning electron microscopy, but no obvious signs of facetting could be detected. The heated sample, however, did show signs of decomposition, as indicated by small droplets of possibly Ga, about 1/2 μm in diameter. The results of these studies are shown in Figure 6. It is worth mentioning that after heating GaAs to closely below its decomposition temperature (~630°C), the surface exhibits a slightly dull appearance which can be correlated with the formation of Ga-droplets. However, the photosensitivities of such surfaces are not adversely affected.

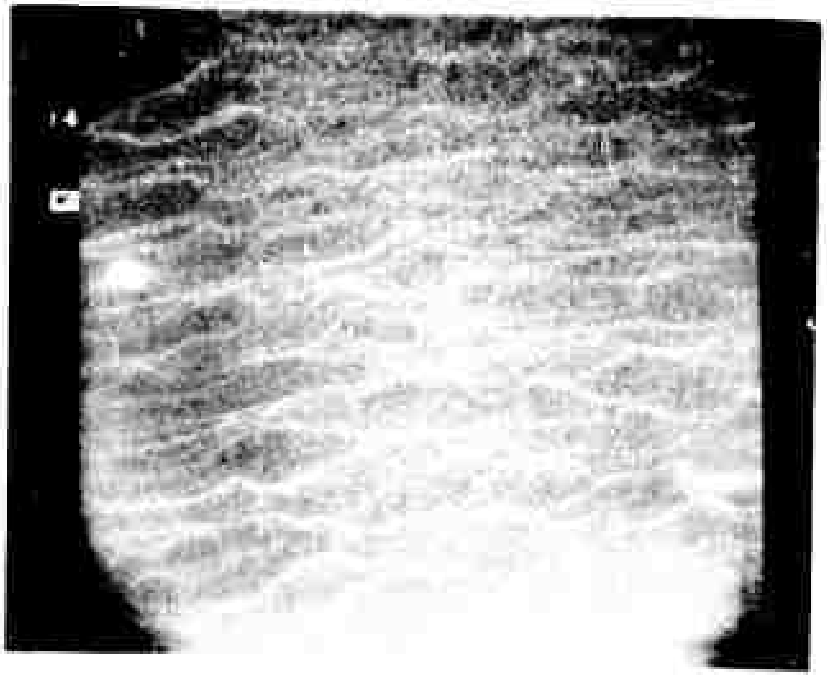

(a)

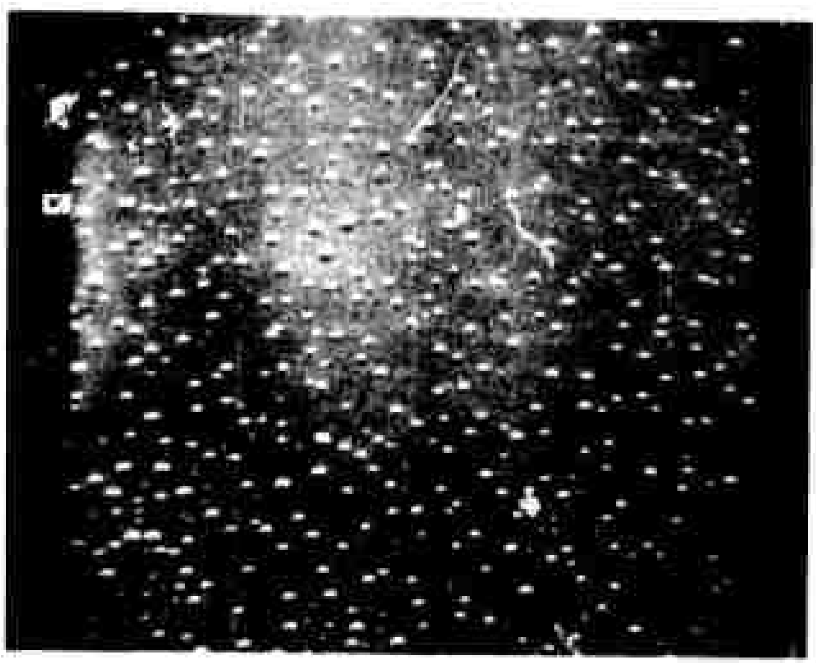

(b)

Figure 6. Scanning electron micrographs of a 100 GaAs surface (a) before and (b) after heating in vacuum to about 600°C.

IV. DIFFUSION LENGTH MEASUREMENTS*

We previously determined the diffusion length in p-type GaAs:Ge on the basis of photoemission measurements (4). However, since this type of material constitutes a major element of the cold-cathode structure, we have now performed additional measurements using more direct techniques. In particular, we were interested in determining the diffusion length in highly doped material ($10^{19}cm^{-3}$). The use of such material is advantageous in reducing the series resistance of the diode and, moreover, in reducing the width of the energy distribution of the emitted electrons (see Figure 4).

The GaAs epitaxial layers were grown in a boat similar to that previously described (6), from solutions of Ga, As, and Ge. Growth was initiated at 900°C, and, in order to minimize doping gradients in the layers, the solution was cooled only a total of 10°C at a rate of 0.25°C/min. The layers (20 to 30 μm thick) were wiped clean at 890°C by pulling the wafer into a bin adjacent to the one containing the Ga solution.

The samples described here were grown from solutions containing Ga/Ge atomic ratios of 10(#1), 100(#2), and 1000(#3). The substrates were (100) oriented semi-insulating ($10^8\Omega$-cm)GaAs:Cr or GaAs:Si wafers with an electron concentration of $2 \times 10^{18}cm^{-3}$. The dislocation density of the latter substrates was < 100 cm^{-2}. Hall measurements of the "comparison" samples grown on the semi-insulating substrates yielded the electron concentrations shown in Table I for samples #1 and #2 which are in good agreement with the values previously reported (7) for material similarly grown. The carrier concentration of sample #3 was determined from C-V measurements of the abrupt p-n junction formed between the epitaxial layer and the substrate. Since material grown from undoped Ga solutions had electron concentrations of about $3 \times 10^{16}cm^{-3}$, sample #3 was significantly compensated by background impurities.

The diffusion length was directly measured by using two techniques. The first method, using the laser beam scan across a beveled p-n junction, is sensitive to surface recombination since the light is strongly absorbed near the surface. The second technique using penetrating α-particles is much less sensitive to the surface condition but is useful under more restrictive conditions.

A. DIFFUSION LENGTH MEASUREMENT USING LASER SCAN

The samples were prepared for laser beam spot scanning by first cleaving bars from the epitaxial wafers on which a Sn-Ni-Au ohmic contact had been applied to the n-type substrate side. The cleaved bars, about 0.5 cm wide and 0.7 cm long, were then lapped at an angle of 1° to the junction along their length. This was followed by a 1% Br-methanol or 5:1:1 sulfuric acid: peroxide:water etch to remove any mechanical damage which may have been introduced.

*The work described in this section was performed in collaboration with M. Ettenberg.

The angle-lapped bar was then placed on a movable stage, and a point contact was made to the p-type epitaxial layers except for the lowest doped sample, #3, where ohmic contact was made to the p-layer with a bonded Au-Zn wire. The connection to the n-side of the junction was made by a mechanical contact between the stage and the ohmic contact to the substrate. In all cases, the large-area angle-lapped p-n junction had good diode I-V characteristics.

The 0.5-mW He-Ne laser beam (λ = 6328 Å) was collimated with a 20 X microscope objective and one auxiliary lens. The optical system, using two 10% mirrors, allowed simultaneous visual examination of the collimated laser spot and the angle-lapped surface. The smallest attainable spot size was 12 μm in diameter. A filter (Corning #1-56) was used to ensure that no infrared radiation emanating from the laser impinged on the sample. The entire experimental setup is shown in Figure 7.

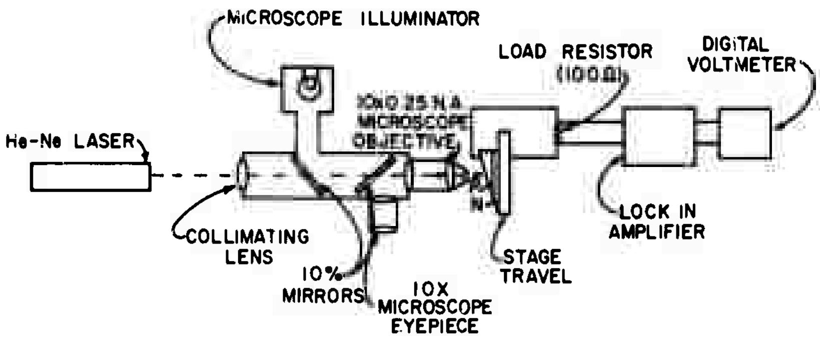

Figure 7. Scanning laser beam method for electron diffusion length measurement.

The diffusion lengths were determined by scanning the laser spot along the angle-lapped specimen and measuring the short-circuit current as a function of distance from the p-n junction at intervals of 25 μm. The p-n junction position was accurately determined by noting a maximum in the short-circuit current as a function of position. From an extrapolation of absorption data for GaAs (8) at 6328 Å, the laser light is attenuated by (1/e) in 0.25 μm. The estimated resolution in the diffusion length value is ~0.5 μm.

The short-circuit current was measured by mechanically chopping the laser beam and using a PAR lock-in amplifier and digital millivoltmeter to determine the voltage across the shorting resistor. Resistors of 1 Ω, 10 Ω, and 100 Ω yielded identical results. The 100-Ω resistor was used for maximum signal. The laser beam was also used to determine the angle of the beveled specimen by measuring the angle between the beams reflected from the angle-lapped surface and a plate parallel to the back of the sample. The error in this measurement was not more than 5%. Microscopic examination of etched cleaved edges showed that the p-n junction was parallel to the back of the sample.

The short-circuit current on a relative scale is plotted in Figure 8 as a function of the p-layer thickness for the specimens studied. The thickness was determined from the measured angle of the beveled surface and the lateral distance from the p-n junction.

The functional relationship between short-circuit current and the p-layer thickness in photodiodes was previously derived (9). For incident light which does not penetrate into the n-side, the short-circuit current I_{SC} is a function of the surface recombination velocity S, the minority-carrier diffusion coefficient D, the minority-carrier diffusion length L, and the absorption coefficient of the incident radiation α ($\sim 10^5 \text{cm}^{-1}$ in this case). For $\alpha x > 1.0$, where x is the p-layer thickness and $\alpha > 1/L$, I_{SC} is given by

$$I_{SC} \propto \frac{1}{\left(\frac{S}{D} + \frac{1}{L}\right) e^{x/L} - \left(\frac{S}{D} - \frac{1}{L}\right) e^{-x/L}} , \tag{3}$$

or

$$I_{SC} \propto \frac{1}{e^{x/L} - Re^{-x/L}} , \tag{4}$$

where

$$R \equiv \frac{\frac{S}{D} - \frac{1}{L}}{\frac{S}{D} + \frac{1}{L}} . \tag{5}$$

For x > L, the first term in the denominator of Eq.(3) predominates, and the slope of the $\ln(I_{SC})$ vs. x plot yields the diffusion length L directly. The L values obtained for four samples studied are shown in Table I. The shape of the curve for $x \leq L$ depends on whether S/D is greater or smaller than 1/L. Having estimated L, R can be obtained by a fit of Eq.(4) to the data in Figure 8. The value of R varies between 1.0 and 0.8, depending on the doping level. Values of D may be estimated by assuming that the mobility of electrons in p-type material is the same as that in n-type of the same carrier density. From the experimental value of R and L and the estimated value of D, a value of S ranging from 8 to 11 x 10^5 cm/sec for the etched GaAs surface was derived and is listed in Table I.

In order to check the reproducibility of the material, two similarly grown 10 Ga:1 Ge samples (#1 and #4) were measured. As shown in Table I, the L values (5.5 and 5.9 μm) were comparable.

B. DIFFUSION LENGTH MEASUREMENT USING α-PARTICLES

Since any measurement technique may contain systematic errors, we checked the diffusion length results with a completely different technique, one developed by Goldstein (10), in which a cleaved p-n junction is scanned with a collimated

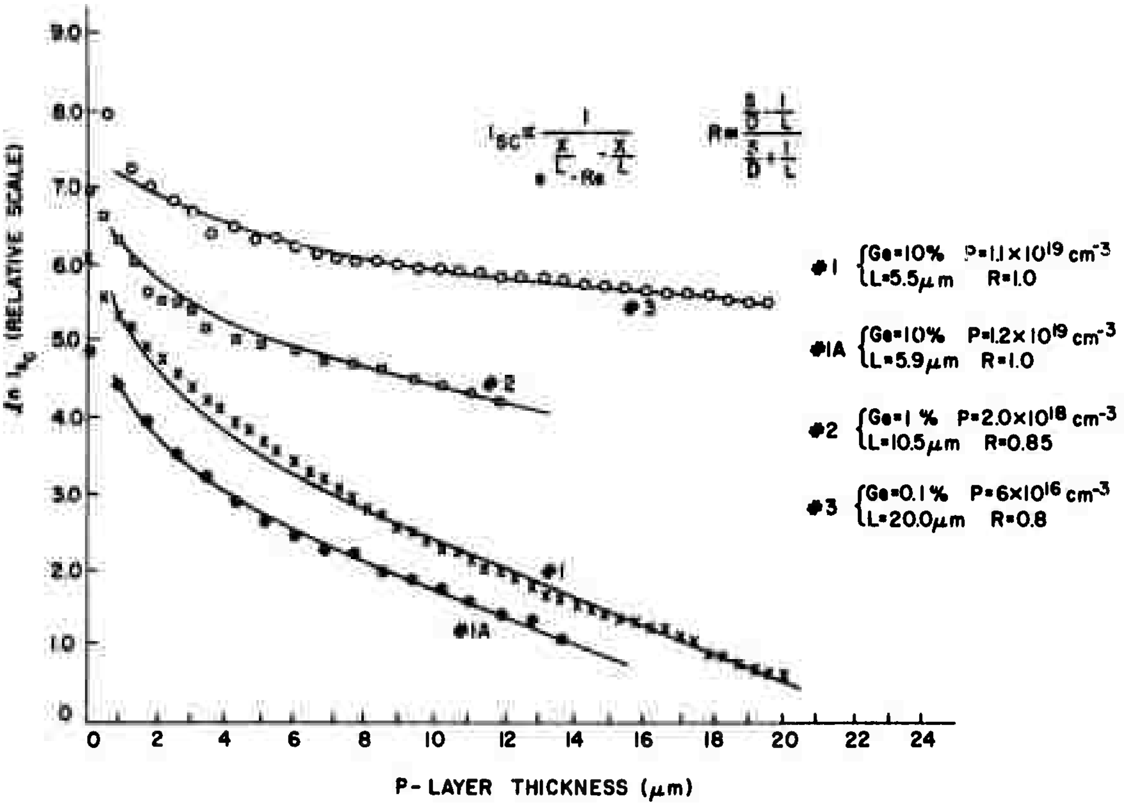

Figure 8. Short-circuit current as a function of the thickness of the p-layer which is illuminated by the laser beam.

beam of α-particles 1 μm in diameter. The main advantage of this method is the large depth of α-particle penetration, 15 μm in GaAs, compared with 1.7 μm for 20-keV electrons, and less than 1 μm for photons with greater than bandgap energy. This large α-particle penetration depth eliminates many of the analysis problems associated with surface recombination.

The diodes employed were made from the same material used for the laser scan measurements described earlier. The material was cleaved into bars 450 μm wide, and then sawed into diodes 120 μm wide and soldered onto headers.

The 5.3-MeV α-particles were obtained from a (Po)210 source about 50 mCi in strength collimated by a 1-μm hole in a 24-μm thick metal diaphragm. The distance x from the junction was varied by means of a differential screw thread having 0.2-μm resolution. The charge collected at the junction was measured with a charge storage amplifier and displayed on an oscilloscope.

The charge q collected by the junction is given by

$$q = q_o \exp\left(- \frac{x}{L} \right) \qquad (6)$$

where q_o is the charge produced by the α-particle at a distance x from the junction for a minority carrier diffusion length L. The charge q is deduced from the maximum height of the envelope of pulses produced by the α-particle beam. The carrier diffusion length L is obtained from the slope of a semi-logarithmic plot of the collected charge q as a function of the distance x. The L values thus derived are listed in Table I and are in very good agreement with those inferred from the laser beam scan method.

TABLE I

Major Material Parameters and Diffusion Length Values in GaAs:Ge

Sample #	Ga/Ge Atomic Ratio in Solution	N_A-N_D (cm^{-3})	Estimated Electron Mobility (cm^2/V-sec)	Diffusion Coefficient D (a) (cm^2/sec)	Diffusion Length L (b) (μm)	(c) (μm)	Surface Recombination Velocity $S \times 10^6$ (cm/sec)
1	10	1.1×10^{19}	1500	40	5.5	5.6	---
2	100	2.0×10^{18}	3500	90	10.5	11.5	1.1
3	1000	6×10^{16}	6500	165	20.0	16.0	0.74
4	10	1.2×10^{19}	---	---	5.9	---	---

(a) Calculated from estimate of electron mobility.

(b) From laser beam scan measurement.

(c) From α-particle scan measurement.

V. OPERATION IN SEALED TUBES

We showed previously that the emission efficiency of a GaAs cold-cathode in a sealed tube stayed practically constant (2.0 to 1.9%) over a period of 2 months (shelf life). This specific tube did not contain any of the features necessary to eliminate contamination of the emitting surface due to electron-stimulated desorption described earlier (1) and, therefore, could not be tested under continuous emission. In the meantime, we have concentrated on achieving *long-term operation* of cathodes in sealed tubes. We constructed a tube to be sealed off, whose main feature was the incorportion of a GaAs anode in order to reduce the contaminating effects of electron-stimulated desorption. Thus far, we have activated in this tube three different samples, but mechanical sample problems prevented the long-term testing of the first two samples. Life testing on the third sample has been started. Simulating sealed-off conditions, we valved-off the tube from the pump and measured a dc emission decrease of only 10% for a period of 15 hours, during which the cathode was operated at an efficiency of about 0.1% with 20-μA total emission and a collector voltage of 30 V. This degradation rate compares favorably with our previous results obtained under dynamic vacuum conditions. It may be anticipated, therefore, that cathode operation will not be adversely affected after sealing the tube.

VI. CONCLUSIONS

The electron energy distribution of a semiconductor cold-cathode based on negative electron affinity was measured for the first time. The half-width of the energy distribution of electrons, emitted from a GaAs-(AlGa)As structure, was found to be 160 meV which is distinctly narrower than that for a conventional thermionic cathode. The measured half-width is in fair agreement with calculations that take into account energy losses suffered by the electrons in the space charge region below the surface.

We have performed a series of photoemission measurements to investigate various surface treatments that might lead to an improved surface escape probability and hence improved cathode efficiency. In addition to ⟨100⟩ GaAs surfaces, we also studied ⟨111B⟩ surfaces which reportedly exhibit higher escape probabilities. Thus far, however, we could not exceed our previous escape probabilities, neither by different surface preparations nor with ⟨111B⟩ surfaces.

Independent diffusion length measurements corroborated our earlier results on the long diffusion lengths in Ge-doped GaAs which is used here as the top layer of our cold-cathode structures. In addition, the diffusion length was measured for higher doping concentrations ($\sim 10^{19} cm^{-3}$) and found to be still rather long (~ 5 μm). The use of this highly doped material in cold-cathodes thus may reduce the series resistance of the diodes as well as the energy spread of the emitted electrons, without a loss in emission efficiency due to reduced diffusion lengths.

After having obtained excellent shelf life of cold-cathode efficiency in a sealed tube (~2% for 2 months) preliminary results on long-term operation in a sealed tube indicate that the cathode degradation rate favorably compares with previous results found in continuously pumped tubes. The transition to sealed tubes, therefore, does not seem to adversely affect cold-cathode operation.

VII. FUTURF PLANS

Further experiments will be needed to clearly establish long-term cold-cathode operation in sealed tubes. At the same time, efforts will be made to incorporate a cold-cathode into an electron-beam-injected transistor (EBIT). For this purpose, a conventional electron gun structure has to be modified to accommodate the semiconductor cold-cathode in place of the thermionic cathode. For this geometry, procedures for mounting and activating the cold-cathode have to be worked out and tested for compatibility with other elements of the device.

REFERENCES

1. H. Schade, H. Nelson, and H. Kressel, Appl. Phys. Letters 20, 385 (1972).
2. D. J. Bartelink, J. L. Moll, and N. I. Meyer, Phys. Rev. 130, 972 (1963).
3. See, for example, J. W. Gewartowski, and H. A. Watson, Principles of Electron Tubes, (D. Van Nostrand, Princeton, N.J., 1965), p.60.
4. H. Schade, H. Nelson, and H. Kressel, Appl. Phys. Letters 18, 121 (1971).
5. L. W. James, G. A. Antypas, J. Edgecumbe, R. L. Moon, and R. L. Bell, J. Appl. Phys. 42, 4976 (1971).
6. H. F. Lockwood and M. Ettenberg, J. Crystal Growth 15, 81 (1972).
7. F. E. Rostoczy, F. Ermanis, I. Hayashi, and B. Schwartz, J. Appl. Phys. 41, 264 (1970).
8. I. Kudman and T. Seidel, J. Appl. Phys. 33, 771 (1962).
9. J. J. Loferski and J. J. Wysocki, RCA Review 22, 38 (1961).
10. B. Goldstein, J. Appl. Phys. 42, 2570 (1971).